Frequency response of a supported thermocouple wire: Effects of axial conduction

G. C. Fralick
Research Sensor Technology Branch, NASA–Lewis Research Center, Cleveland, Ohio 44135

L. J. Forney
School of Chemical Engineering, Georgia Institute of Technology, Atlanta, Georgia 30332

(Received 18 January 1993; accepted for publication 10 August 1993)

Theoretical expressions are derived for the steady-state frequency response of a supported thermocouple wire. In particular, the effects of axial heat conduction are demonstrated for both a supported one material wire and a two material wire with unequal material properties across the junction. For the case of a one material supported wire, an exact solution is derived which compares favorably with an approximate expression that only matches temperatures at the support junction. Moreover, for the case of a two material supported wire, an analytical expression is derived that closely correlates numerical results.

I. INTRODUCTION

The evaluation of jet engine performance and fundamental studies of combustion phenomena depend on the measurement of turbulent fluctuating temperatures of the gas within the engine.[1] Historically, these temperatures have been measured with thermocouples. The design of a thermocouple represents a compromise between accuracy, ruggedness and rapidity of response.

For example, the measurement of fluctuating temperatures in the high speed exhaust of a gas turbine engine combustor is required to characterize the local gas density gradients or convective heat transfer.[2] Although thermocouples are suitable for the measurement of high frequency temperature fluctuations (<1 kHz) in a flowing gas or liquid, the measured signal must be compensated since the frequency of the time dependent fluid temperature is normally much higher than the natural frequency of the thermocouple probe.[3] Moreover, the amplitude and phase angle of the thermocouple response may be attenuated by axial heat conduction for rugged thermocouples of finite length.[4–7]

In the present study, the theoretical steady-state frequency response of a supported thermocouple wire has been calculated to include the effects of axial heat conduction. These solutions, that represent an extension of earlier work,[8] are derived for both a supported thermocouple wire with equal physical properties across the junction (e.g., roughly the same thermoconductivity, etc.) and a supported wire with unequal properties across the junction. Solutions are presented in the form of the amplitude ratio and phase angle for both cases and these results have been compared favorably with experimental data.[7]

II. THEORY FOR ONE MATERIAL THERMOCOUPLE

The steady-state frequency response of a thermocouple wire will be developed with the following assumptions: (a) the amplitude of the fluctuating fluid temperature is small relative to the mean absolute temperature, (b) the thermocouple dimensions are small relative to the size of the turbulent eddies or enclosure dimensions, (c) radial temperature gradients in a wire cross section can be neglected, and (d) radiative heat transfer can be neglected relative to conduction and convection.

In this section the geometry of Fig. 1 is considered where the material properties of thermal conductivity k, specific heat c and wire density ρ are assumed to be equal on both sides of the thermocouple junction. If the probe is immersed in a flowing fluid, the expression for the local conservation of energy in the thermocouple wire becomes[3]

$$\frac{\partial T_w}{\partial t}=\alpha\frac{\partial^2 T_w}{\partial x^2}+\frac{4h}{\rho c D}(T_g-T_w), \tag{1}$$

where $\alpha=k/\rho c$ is the thermal diffusivity of the wire, T_g is the ambient fluid temperature, h is the convective heat transfer coefficient, D is the wire diameter and T_w is the local wire temperature measured along the axis at a distance x from the centerline (Fig. 1.)

The wire and fluid temperatures are measured relative to the mean fluid temperature T_0. The ambient fluid temperature is taken to be a mean temperature together with a sinusoidal varying deviation from the mean,

$$T_g(t)=T_0+T_f e^{i\omega t}, \tag{2}$$

where ω is the angular frequency of the ambient temperature. Since Eq. (1) is linear, we now seek a solution for the local wire temperature of the form[9]

$$T_w=T_0+\mathrm{T}_\omega(x)e^{i\omega t}. \tag{3}$$

Referencing all temperatures with respect to the mean gas temperature T_0 and normalizing with respect to the amplitude of the fluctuating ambient fluid temperature T_f, one defines a local normalized steady-state frequency response $\mathrm{T}(x)$ for the thermocouple wire of the form

$$\frac{T_w-T_0}{\mathrm{T_f}}=\frac{\mathrm{T}_\omega(x)e^{i\omega t}}{\mathrm{T_f}}=\mathrm{T}(x)e^{i\omega t}. \tag{4}$$

Substituting Eqs. (2) and (3) into Eq. (1), one obtains an ordinary differential equation of the form

 0034-6748/93/64(11)/3236/9/$6.00

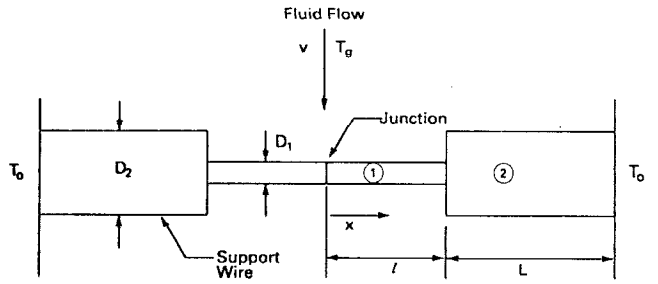

FIG. 1. Schematic of one material supported wire.

$$i\omega T=\alpha\frac{d^2T}{dx^2}+\omega_n(1-T), \tag{5}$$

where $T=\mathbf{T}(x)$ is the frequency response and the vector notation will be dropped for simplicity. Thus, for the geometry of Fig. 1, one seeks a solution to the nonhomogeneous linear second order differential equation for the dependent variable T of the form[8]

$$\gamma T''-G(\omega)T=-1. \tag{6}$$

The general solution to Eq. (6) can be written in the form[9]

$$T(x)=A\sinh qx+B\cosh qx+\frac{1}{G(\omega)}, \tag{7}$$

where the parameters in Eqs. (5) and (6) are defined as

$$\omega_n=\frac{4h}{\rho cD},\quad \gamma=\frac{\alpha}{\omega_n},\quad G(\omega)=1+i\left(\frac{\omega}{\omega_n}\right), \tag{8}$$

while in Eq. (7) the constants A and B are complex, $1/G(\omega)$ represents the particular solution and the parameter

$$q=\sqrt{\frac{G(\omega)}{\gamma}}.$$

A. Approximate solution

Assuming that the material properties are constant across the junction and that the wire diameters are D_1 and D_2 in regions 1 and 2, respectively, Eq. (6) is subject to the boundary conditions

$$T_1(l)=T_2(l)=T_a, \tag{9a}$$

$$T_2(l+L)=0. \tag{9b}$$

In this case, we seek a simple approximate solution that neglects the heat transfer at the interface between regions 1 and 2 at $x=\pm l$ where the parameters in Eqs. (5) and (6) are defined in terms of the wire diameters in each region. A similar approach will be used in a later section to obtain an approximate solution for the case in which the material properties of the two elements of the thermocouple are distinctly different. Hence, in region 1

$$\omega_1=\frac{4h_1}{\rho cD_1},\quad \gamma_1=\frac{\alpha}{\omega_1},\quad G_1(\omega)=1+i\left(\frac{\omega}{\omega_1}\right), \tag{10}$$

where ω_1 is the natural frequency of the wire in region 1 of Fig. 1.

The solution to Eq. (6) for the one material wire on both sides of the junction in region 1 can be written in the form

$$T_1(x)=A_1\sinh q_1x+B_1\cosh q_1x+\frac{1}{G_1(\omega)}. \tag{11}$$

Substituting $x=\pm l$ in Eq. (11), the boundary conditions in Eq. (9) yield values for the constants

$$A_1=0,\quad B_1=\frac{1}{\cosh q_1l}\left(T_a-\frac{1}{G_1}\right). \tag{12}$$

Thus, one obtains a steady-state temperature distribution for the wire in region 1 of Fig. 1 in the form

$$T_1(x)=\frac{1}{G_1}\left(1-\frac{\cosh q_1x}{\cosh q_1l}\right)+T_a\left(\frac{\cosh q_1x}{\cosh q_1l}\right). \tag{13}$$

We now seek a solution in region 2 that satisfies the boundary conditions of Eq. (9). Since the temperature is symmetric about $x=0$, it is convenient to define a continuous steady-state temperature distribution for the large wire of diameter D_2 over the entire region $-(l+L)\leqslant x\leqslant(l+L)$ or

$$T_2(x)=\frac{1}{G_2}\left(1-\frac{\cosh q_2x}{\cosh q_2(l+L)}\right). \tag{14}$$

Since $T_a=T_2(l)$, one obtains the boundary value from Eq. (14),

$$T_a=\frac{1}{G_2}\left(1-\frac{\cosh q_2l}{\cosh q_2(l+L)}\right). \tag{15}$$

Substituting the value for T_a at $x=l$ of Eq. (15) into Eq. (13), the approximate temperature distribution in region 1 becomes

$$T_1(x)=\frac{1}{G_1}\left(1-\frac{\cosh q_1x}{\cosh q_1l}\right)+\frac{1}{G_2}\left(1-\frac{\cosh q_2l}{\cosh q_2(l+L)}\right)\frac{\cosh q_1x}{\cosh q_1l}. \tag{16}$$

Thus, the approximate frequency response at the thermocouple junction ($x=0$) for the one material wire becomes

$$T_1(0)=\frac{1}{G_1}\left(1-\frac{1}{\cosh q_1l}\right)+\frac{1}{G_2}\left(1-\frac{\cosh q_2l}{\cosh q_2(l+L)}\right)\frac{1}{\cosh q_1l}. \tag{17}$$

The steady-state behavior at the thermocouple junction $x=0$ is normally characterized graphically in the form

$$T(0)=|T(0)|e^{i\Phi}, \tag{18}$$

where $|T(0)|$ is the amplitude ratio and Φ is the phase angle. In the latter case, the phase angle in degrees is

$$\Phi=57.3\tan^{-1}\left(\frac{\mathrm{Im}\,T(0)}{\mathrm{Re}\,T(0)}\right), \tag{19}$$

where Im$[T(0)]$ and Re$[T(0)]$ are the imaginary and real parts of $T(0)$, respectively.

B. Exact solution

If the boundary conditions listed in Eq. (9) include equal rates of conductive heat transfer at the interface between the thermocouple and support wires at $x=\pm l$, the exact solution is subject to

$$T_1(l)=T_2(l), \tag{20a}$$

$$kD_1^2\frac{dT_1(l)}{dx}=kD_2^2\frac{dT_2(l)}{dx}, \tag{20b}$$

$$T_2(l+L)=0. \tag{20c}$$

Since the solution to Eq. (6) in region 1 is of the form

$$T_1(x)=A_1\sinh q_1x+B_1\cosh q_1x+\frac{1}{G_1}, \tag{21}$$

where by symmetry $T_1(l)=T_1(-l)$, one obtains $A_1=0$. Thus, the form of the solution in region 1 becomes

$$T_1(x)=B_1\cosh q_1x+\frac{1}{G_1}. \tag{22}$$

For region 2, where the spatial coordinate is in the range $l\leqslant x\leqslant(l+L)$, it is convenient to write

$$T_2(x)=A_2\sinh q_2(l+L-x)+B_2\cosh q_2(l+L-x)+\frac{1}{G_2}. \tag{23}$$

From the boundary condition $T_2(l+L)=0$, one obtains $B_2=-1/G_2$ or the form of the solution in region 2 becomes

$$T_2(x)=A_2\sinh q_2(l+L-x)+\frac{1}{G_2}[1-\cosh q_2(l+L-x)]. \tag{24}$$

Substituting Eqs. (22) and (23) into boundary condition (20a), one obtains a linear equation for the constants B_1, A_2, or

$$B_1\cosh q_1l-A_2\sinh q_2L=\frac{1}{G_2}[1-\cosh q_2L]-\frac{1}{G_1}. \tag{25}$$

Similarly, substituting Eqs. (22) and (23) into boundary condition (20b), one obtains a second linear equation for B_1, A_2, or

$$B_1Q\sinh q_1l+A_2\cosh q_2L=\frac{1}{G_2}\sinh q_2L, \tag{26}$$

where the complex constant Q is defined as

$$Q=\frac{D_1^2q_1}{D_2^2q_2}. \tag{27}$$

Solving Eqs. (25) and (26) for B_1 and A_2, one obtains the determinate system

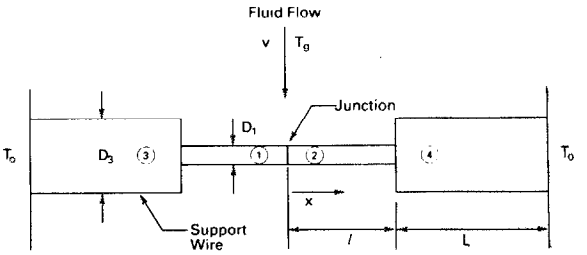

FIG. 2. Schematic of two material supported wire.

$$B_1=\frac{\begin{vmatrix}\frac{1}{G_2}(1-\cosh q_2L)-\frac{1}{G_1} & -\sinh q_2L\\ \frac{1}{G_2}\sinh q_2L & \cosh q_2L\end{vmatrix}}{\mathrm{DET}} \tag{28}$$

and

$$A_2=\frac{\begin{vmatrix}\cosh q_1l & \frac{1}{G_2}(1-\cosh q_2L)-\frac{1}{G_1}\\ Q\sinh q_1l & \frac{1}{G_2}\sinh q_2L\end{vmatrix}}{\mathrm{DET}}, \tag{29}$$

where the determinate in the denominator is equal to

$$\mathrm{DET}=\cosh q_1l\cosh q_2L+Q\sinh q_1l\sinh q_2L. \tag{30}$$

Thus, solving for the constants B_1 and A_2 from Eqs. (28) and (29) and substituting B_1 into Eq. (22), one obtains an exact expression for the steady-state temperature distribution in the form

$$T_1(x)=\frac{\left(\frac{1}{G_2}(\cosh q_2L-1)-\frac{1}{G_1}\cosh q_2L\right)\cosh q_1x}{\cosh q_1l\cosh q_2L+Q\sinh q_1l\sinh q_2L}+\frac{1}{G_1}. \tag{31}$$

Thus, the steady-state frequency response at the thermocouple junction $x=0$ becomes

$$T(0)=\frac{\frac{1}{G_2}(\cosh q_2L-1)-\frac{1}{G_1}\cosh q_2L}{\cosh q_1l\cosh q_2L+Q\sinh q_1l\sinh q_2L}+\frac{1}{G_1}. \tag{32}$$

III. THEORY FOR TWO MATERIAL THERMOCOUPLE

Certain types of thermocouples have distinctly different material properties across the junction. For example, a copper–constantan thermocouple has a thermal conductivity on the copper side that is more than an order of magnitude larger than constantan. In this case, the expressions developed in the previous section for the frequency response are in error since unequal material properties would provide an asymmetric temperature profile.

Referring to Fig. 2, the thermocouple schematic now

has four distinct regions that are distinguished by either different wire diameters or physical properties. For example, on the left-hand side of the schematic of Fig. 1 the thermal conductivity, density and specific heat have the values k_1, ρ_1, and c_1, respectively, while on the right-hand side of the schematic the material properties are k_2, ρ_2, and c_2.

A. Temperature distribution for small wire

Since the differential equation describing the steady-state frequency response Eq. (6) applies to all regions of the schematic of Fig. 1, the steady-state frequency response in regions 1 and 2 are given, respectively, by the expressions

$$T_1(x)=A_1 \sinh q_1 x+B_1 \cosh q_1 x+\frac{1}{G_1}, \tag{33}$$

$$T_2(x)=A_2 \sinh q_2 x+B_2 \cosh q_2 x+\frac{1}{G_2}. \tag{34}$$

Here, the four constants designated by A and B in Eqs. (33) and (34) are determined by the four boundary conditions

$$T_1(0)=T_2(0), \tag{35a}$$

$$k_1 D_1^2 \frac{dT_1(0)}{dx}=k_2 D_1^2 \frac{dT_2(0)}{dx}, \tag{35b}$$

$$T_1(-l)=T_a, \tag{35c}$$

$$T_2(l)=T_b. \tag{35d}$$

Solving for the four values of the constants designated by A and B in Eqs. (33) and (34), one obtains an expression for the steady-state temperature distribution in region 1 of the form

$$\begin{aligned} T_1(x)=&\frac{1}{G_1}+\left\{\sinh q_1(x+l)\left[\left(\frac{1}{G_2}-\frac{1}{G_1}\right)\cosh q_2 l\right.\right. \\ &\left.+\left(T_b-\frac{1}{G_2}\right)\right]+\left(T_a-\frac{1}{G_1}\right) \\ &\times[Q_t \cosh q_1 x \sinh q_2 l \\ &\left.-\sinh q_1 x \cosh q_2 l]\right\}\left(\frac{1}{\Delta_1}\right) \end{aligned} \tag{36a}$$

and in region 2

$$\begin{aligned} T_2(x)=&\frac{1}{G_2}+\left\{-Q_t \sinh q_2(l-x)\left[\left(\frac{1}{G_2}-\frac{1}{G_1}\right)\cosh q_1 l\right.\right. \\ &\left.-\left(T_a-\frac{1}{G_1}\right)\right]+\left(T_b-\frac{1}{G_2}\right)[\cosh q_2 x \sinh q_1 l \\ &\left.+Q_t \cosh q_1 l \sinh q_2 x]\right\}\left(\frac{1}{\Delta_1}\right). \end{aligned} \tag{36b}$$

Here, it should be noted that the two functions above can be obtained from each other by interchanging the subscripts 1 and 2, the values a and b and by changing the sign of x. Also, in Eqs. (36a) and (36b) the parameters

$$\Delta_1=Q_t \cosh q_1 l \sinh q_2 l+\cosh q_2 l \sinh q_1 l,$$

and

$$Q_t=\frac{k_1 q_1}{k_2 q_2}.$$

B. Temperature distribution for large wire

In this section a solution is sought for the large wire in regions 3 and 4 of the schematic of Fig. 2. To simplify the analysis, a continuous solution is derived for the steady-state frequency response over the entire region $-(l+L)\leqslant x\leqslant(l+L)$. This solution must satisfy the boundary conditions

$$T_3(0)=T_4(0), \tag{37a}$$

$$k_1 D_3^2 \frac{dT_3(0)}{dx}=k_2 D_3^3 \frac{dT_4(0)}{dx}, \tag{37b}$$

$$T_3(-l-L)=0, \tag{37c}$$

$$T_4(l+L)=0. \tag{37d}$$

In principle, it is now possible to derive a continuous solution for $T_3(x)$ over the range $-(l+L)\leqslant x\leqslant 0$ and for $T_4(x)$ over the range $0\leqslant x\leqslant(l+L)$. These solutions are obtained from Eqs. (36a) and (36b) by renumbering the subscripts $1\rightarrow 3$ and $2\rightarrow 4$, redefining the parameters $l\rightarrow l+L$ and setting the boundary conditions $T_a=T_b=0$. Moreover, the boundary condition $T_a=T_3(-l)$ is obtained from the resulting expression for $T_3(x)$ by substituting $x=-l$ while the boundary condition $T_b=T_4(l)$. Thus, one obtains values for T_a, T_b that appear in Eqs. (36a) and (36b) in the form

$$\begin{aligned} T_a=&\frac{1}{G_3}+\left\{\sinh q_3 L\left[\left(\frac{1}{G_4}-\frac{1}{G_3}\right)\cosh q_4(l+L)-\frac{1}{G_4}\right]\right. \\ &-\frac{1}{G_3}[Q_s \cosh q_3 l \sinh q_4(l+L) \\ &\left.+\cosh q_4(l+L)\sinh q_3 l]\right\}\left(\frac{1}{\Delta_2}\right) \end{aligned} \tag{38}$$

and

$$\begin{aligned} T_b=&\frac{1}{G_4}+\left\{Q_s \sinh q_4 L\left[\left(\frac{1}{G_3}-\frac{1}{G_4}\right)\cosh q_3(l+L)-\frac{1}{G_3}\right]\right. \\ &-\frac{1}{G_4}[\cosh q_4 l \sinh q_3(l+L) \\ &\left.+Q_s \cosh q_3(l+L)\sinh q_4 l]\right\}\left(\frac{1}{\Delta_2}\right). \end{aligned} \tag{39}$$

Here, the parameters are defined as

$$\begin{aligned} \Delta_2=&Q_s \cosh q_3(l+L)\sinh q_4(l+L) \\ &+\cosh q_4(l+L)\sinh q_3(l+L) \end{aligned}$$

TABLE I. Properties of one material wire (type B).

Dimensions (cm)				
D_1	D_2	D_2/D_1	l	L
0.025	0.05	2	0.2	0.35
0.0076[a]	0.038	5	0.1	0.2

Average properties of type B		Gas properties
$\rho c\left(\frac{\mathrm{J}}{\mathrm{cm^3\,K}}\right)$	$\alpha\left(\frac{\mathrm{cm^2}}{\mathrm{s}}\right)$	$T_0=900$ K $M=0.26$ $P=1$ atm
3.8	0.22	

[a] $\omega_1=32.9\ \mathrm{s}^{-1}$.

and

$$Q_s=\frac{k_1 q_3}{k_2 q_4}.$$

C. Frequency response

The steady-state frequency response for the two material supported thermocouple is obtained from Eq. (36a) or (36b) by setting $x=0$:

$$T(0)=\frac{1}{\Delta_1}\left[Q_t \sinh q_2 l\left(T_a+\frac{1}{G_1}(\cosh q_1 l-1)\right)+\sinh q_1 l\left(T_b+\frac{1}{G_2}(\cosh q_2 l-1)\right)\right], \tag{40}$$

where T_a and T_b are given by Eqs. (38) and (39).

It should be noted that the steady-state frequency response Eq. (40) provides a wire temperature that is continuous everywhere and conserves the heat flux at the junction $x=0$. This represents an approximate solution since the heat flux at the interface between the large and small wires $x=\pm l$ has been neglected.

IV. RESULTS

The amplitude ratio and phase angle of the thermocouple frequency response were plotted graphically for the case of a one material wire in the schematic of Fig. 1. In this case, average properties of a type B or Pt/6% Rh–Pt/30% Rh were used since the material properties were nearly equal across the thermocouple junction. The wire dimensions, properties and gas conditions are listed in Table I.[10]

The amplitude ratio and phase angle were also plotted for a two material thermocouple wire in the schematic of Fig. 2. In this case, a type B thermocouple described in Table I was used in addition to a type T or copper–constantan described in Table II.[10]

The form of the convective heat transfer coefficient h that appears in the computation of the natural frequency ω_n defined in Eq. (8) was determined from the expression[3]

$$\mathrm{Nu}=0.485\ \mathrm{Re}^{1/2}\ \mathrm{Pr}^{1/3},$$

where $\mathrm{Nu}(=hD/k_f)$ is the Nusselt number, k_f is the thermal conductivity of the ambient fluid, $\mathrm{Pr}(=\upsilon_f/\alpha)$ is the Prandl number, and $\mathrm{Re}(=\upsilon D/\upsilon_f)$ is the Reynolds number

TABLE II. Properties of two material wire.

Dimensions (cm)					
D_1	D_2	D_2/D_1	l	L	Air properties
0.0076	0.038	5	0.1	0.2	$T_0=300$ K $P=1$ atm $V=50$ m/s

	Properties of type B	
	$\rho c\left(\frac{\mathrm{J}}{\mathrm{cm^3\,K}}\right)$	$\alpha\left(\frac{\mathrm{cm^2}}{\mathrm{s}}\right)$
Pt–6% Rh	2.73	0.238
Pt–30% Rh	2.86	0.190
Average	2.8	0.214

	Properties of type T	
	$\rho c\left(\frac{\mathrm{J}}{\mathrm{cm^3\,K}}\right)$	$\alpha\left(\frac{\mathrm{cm^2}}{\mathrm{s}}\right)$
Copper	3.44	1.16
Constantan	3.48	0.067
Average	3.46	0.614

Region	Wire location Type B	Type T
1	Pt–6% Rh	Copper
2	Pt–30% Rh	Constantan

of the thermocouple wire. Here, υ and υ_f are the fluid velocity and kinematic viscosity, respectively. It should be noted that the convective heat transfer coefficient $h\propto D^{-1/2}$ and the natural frequency of a thermocouple wire for given material properties $\omega_n\propto D^{-3/2}$.

A. Useful criterion

The approximate expression for the frequency response of a supported one material wire consists of two terms as given by Eq. (17). The first term represents the exact result illustrating the effects of axial heat conduction for a one material wire of uniform diameter with no support ($L=0$) as previously derived by Chomiak and Niedzialek[11] and Forney and Fralick.[8] The first term of Eq. (17) is

$$T_1(0)=\frac{1}{G_1}(1-\mathrm{sech}\ q_1 l). \tag{41}$$

Here, the coefficient $1/G_1$ represents the first order response for a uniform wire of infinite length ($l\to\infty$) while the term $\mathrm{sech}(q_1 l)$ is the correction due to axial heat conduction.

The second term of Eq. (17) is a useful estimate of the effect of the support legs on the frequency response. Moreover, a useful criterion in practice to evaluate the magnitude of the suggested corrections due to axial heat conduction can be derived from Eq. (41). One must determine the real part of the error written in the form

$$\frac{1/G_1-T_1(0)}{1/G_1}=\mathrm{sech}\ q_1 l\simeq 2e^{-q_1 l}. \tag{42}$$

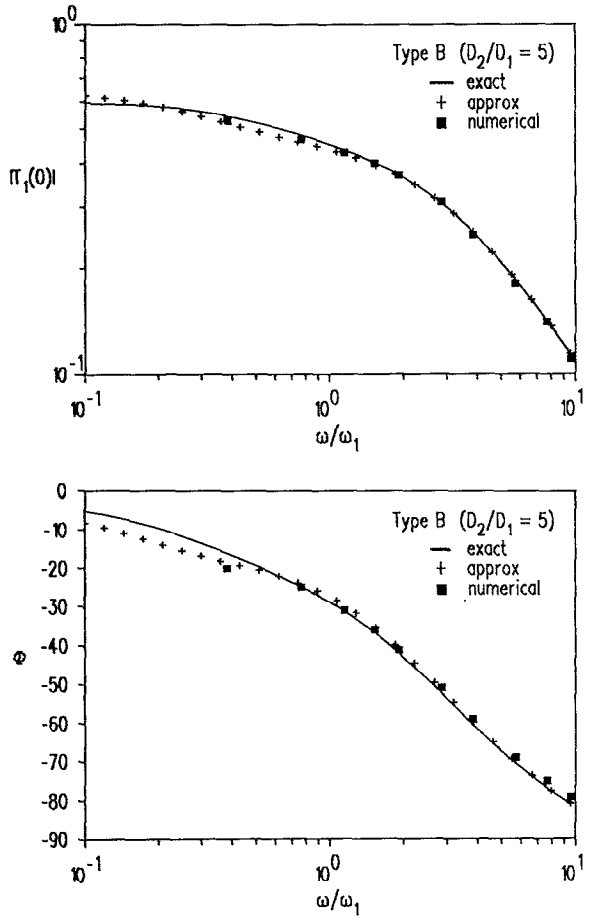

FIG. 3. Amplitude ratio vs angular frequency for one material wire. Lower graph is phase angle vs angular frequency for one material wire. Solid line is exact solution Eq. (32); crosses are approximate solution Eq. (17).

Thus, the maximum error in the amplitude ratio due to axial conduction occurs at a frequency $\omega \to 0$ or

$$\text{error} \simeq 2e^{-l/\sqrt{\gamma_1}}. \tag{43}$$

For example, if $l/\sqrt{\gamma_1}=3.7$ the maximum error in the amplitude ratio is 5% relative to the expected amplitude ratio for a thermocouple wire of infinite length.

B. One material thermocouple

The amplitude ratio $|T(0)|$ at the wire junction for the steady-state frequency response derived from Eqs. (17) and (32) is shown in Fig. 3. This assumes a type B thermocouple wire with the dimensions listed in Table I. In this case, the average material properties listed in Table I were used since the one material theory assumes that the properties of the thermocouple wire are uniform across the junction. It is evident in Fig. 3 that the amplitude ratio derived from the approximate expression Eq. (17) is nearly identical to the exact derivation Eq. (32). Thus, it appears that the conservation of heat flux at the interface between the small and large wires of the schematic of Fig. 1 is of secondary importance.

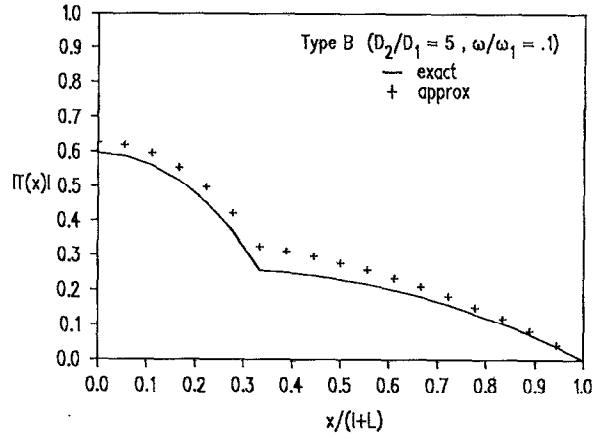

FIG. 4. Amplitude ratio vs distance for one material wire. Solid line is derived from Eqs. (24) and (31). Crosses are derived from Eqs. (14) and (16).

Also included in Fig. 3 are the numerical computations of Stocks.[12] These solutions represent explicit finite difference solutions to the one dimensional unsteady heat transfer equation as shown in Eq. (1). The small deviation of the numerical results from the exact solution at low frequency in Fig. 3 is apparently due to the unsteady character of the numerical results. Similar computations of the phase angle Φ for the type B thermocouple are represented in Fig. 3. As indicated, the phase angle varies over the range $0 \geqslant \Phi \geqslant -\pi/2$ and approaches the lower limit of $-\pi/2$ for large frequencies $\omega/\omega_n \gg 1$.

The spacial variation of the amplitude ratio $|T(x)|$ derived from Eqs. (17) and (32) is plotted in Fig. 4. These computations were made at an angular frequency of $\omega/\omega_n=0.1$ for the type B thermocouple. As evident in Fig. 4, the difference between the exact and approximate expression is somewhat exaggerated at a very low frequency. Nevertheless, the error represented by the approximate solution is less than 7% over the length of the thermocouple. As stated earlier, matching the heat flux at the interface between the small and large wire at $x=\pm l$ in the schematic of Fig. 1 appears to be of secondary importance in relation to providing a continuous temperature profile along the wire.

The amplitude ratio $|T(0)|$ and phase angle Φ are also plotted in Fig. 5 from the steady-state frequency response represented by Eqs. (17) and (32). These results represent a type B thermocouple with a smaller diameter ratio $D_2/D_1=2$ (see Table I for dimensions). As indicated in Fig. 5, the approximate and exact solutions represent comparable results in all three cases. Thus, the diameter ratio of the large and small wire appears to have little effect in the favorable comparison between the approximate and exact solutions representing the one material steady-state frequency response.

The approach used for the approximate solution to the one material wire (i.e., neglecting heat transfer at the wire–support junction) was also used to determine the frequency response of a two material wire as shown in Sec. III. The

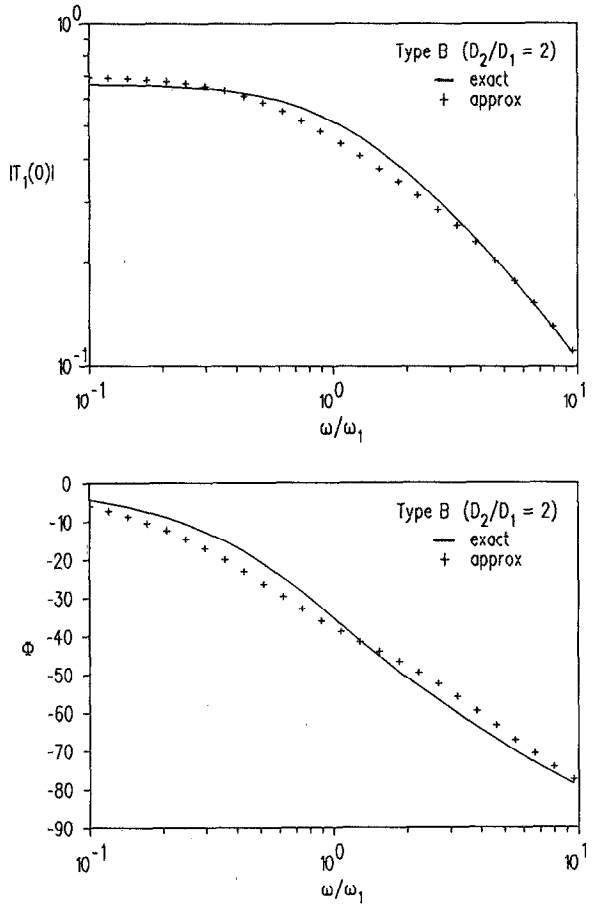

FIG. 5. Amplitude ratio vs angular frequency for one material wire. Lower graph is phase angle vs angular frequency for one material wire. Solid line is Eq. (32). Crosses are Eq. (17).

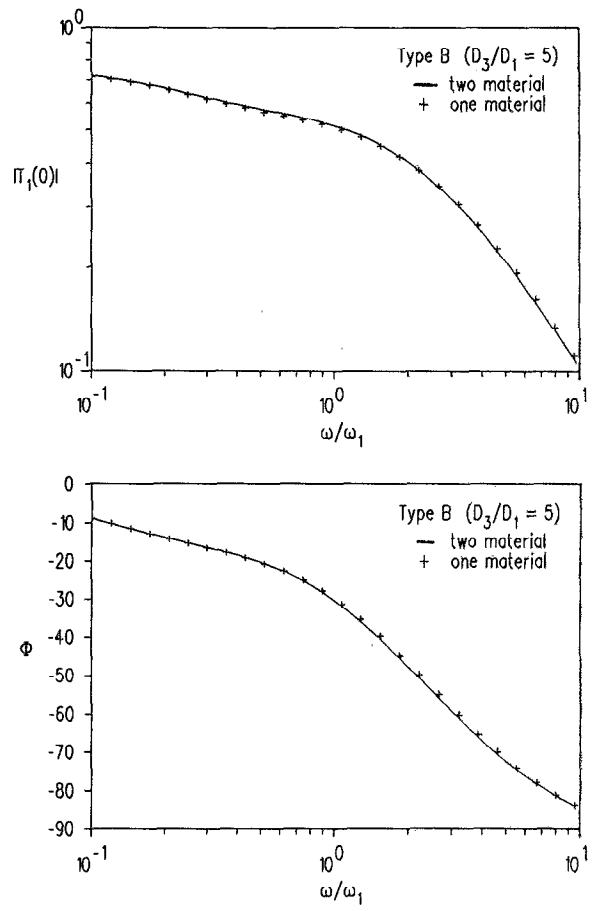

FIG. 6. Amplitude ratio vs angular frequency for two material wire. Lower graph is phase angle vs angular frequency for two material wire. Solid line is Eq. (40). Crosses are approximate one material solution Eq. (17).

exact solution to the two material wire would require the simultaneous and formidable solution of eight equations.

C. Two material thermocouple

The amplitude ratio $|T(0)|$ at the wire junction for the steady-state frequency response derived from Eqs. (17) and (40) is shown in Fig. 6. This assumes a type B thermocouple wire with the dimensions listed in Table II. In this case, the average material properties listed in Table II were used for the amplitude of the frequency response derived from the one material solution of Eq. (17). Also plotted in Fig. 6 is the amplitude ratio derived from the two material solution of Eq. (40). In the latter case, the individual material properties listed in Table II were used.

As expected, the amplitude ratio for the steady-state frequency response of a type B thermocouple is nearly identical with either the one material or two material approximate solutions. This is a consequence of roughly equal material properties across the junction for type B thermocouples. This plot also validates the two material approximate solution Eq. (40) and the values of the boundary conditions for T_a and T_b substituted from Eqs. (38) and (39). The same conclusion can be drawn with respect to the phase angle Φ, shown in Fig. 6.

The steady state amplitude ratio $|T(0)|$ for a type T thermocouple is plotted in Fig. 7 using Eqs. (17) and (40). The dimensions and material properties are listed in Table II. The average material properties listed in Table II were used to compute the amplitude ratio of the frequency response with the one material solution, Eq. (17). Also plot-

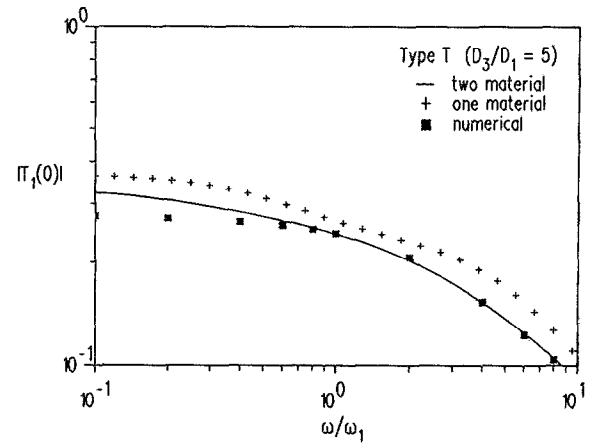

FIG. 7. Amplitude ratio vs angular frequency for two material wire. Solid line is Eq. (40). Crosses are approximate one material solution Eq. (17).

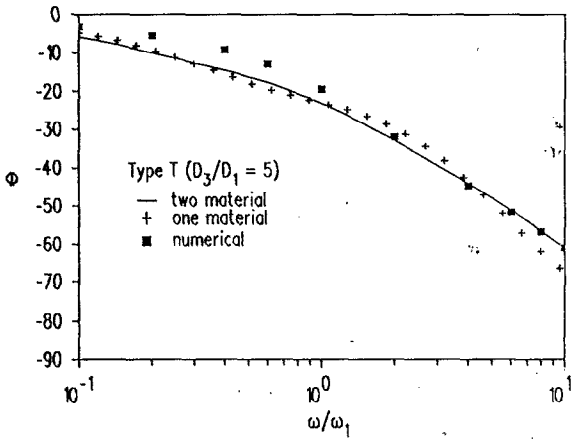

FIG. 8. Phase angle vs angular frequency for two material wire. Solid line is Eq. (40). Crosses are approximate one material solution Eq. (17).

ted in Fig. 7 is the amplitude ratio derived from the two material solution, Eq. (40). In the latter case, the individual material properties also listed in Table II were used.

As indicated in Fig. 7, the amplitude ratio for the approximate one material steady-state frequency response of a type T thermocouple is distinctly different from the two material approximate solution. This is a consequence of unequal material properties across the junction for the type T thermocouple. Also shown in Fig. 7 is a numerical solution of the second order ordinary differential equation for the temperature, Eq. (6). The numerical finite difference solution of the boundary value problem of Eq. (6) matches both the temperature and heat flux at $x=0$ and $x=\pm l$ in the schematic of Fig. 2. It is clear from Fig. 7 that the approximate two material analytical solution, Eq. (40), is in good agreement with the numerical results despite some differences at low frequencies $\omega/\omega_1<0.04$. Similar results are indicated for the phase angle Φ in Fig. 8.

The spacial variation of the amplitude ratio $|T(x)|$ derived from Eqs. (17) and (40) is graphed in Fig. 9. These computations were made at an angular frequency of $\omega/\omega_1=0.1$ for the type T thermocouple. As evident in Fig. 9, the two material solution derived from Eq. (40) accurately represents the features of the asymmetry associated with a type T thermocouple. In particular, the relatively large resistance to axial heat conduction in the constantan wire on the right of the junction is reflected in the larger values of the amplitude ratio $|T(x)|$. Also shown in Fig. 9 is the approximate one material solution represented by Eq. (17). In the latter case, the average values for the material properties of a type T thermocouple were used as listed in Table II. Therefore, one can conclude that for thermocouples whose material properties on either side of the junction are markedly different, the two material solution developed in this paper is a substantial improvement in accuracy both in frequency response and in temperature distribution along the wire.

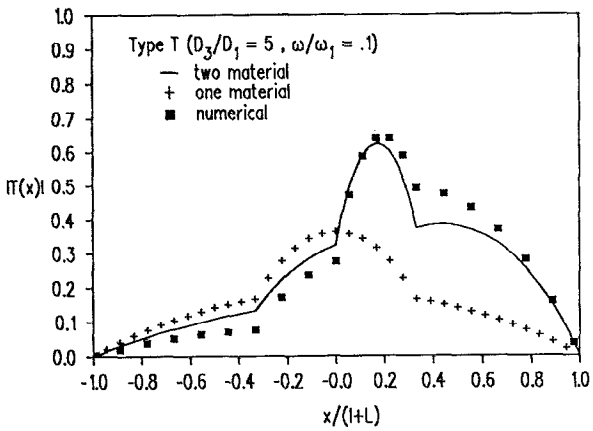

FIG. 9. Amplitude ratio vs distance for two material wire. Solid line derived from Eqs. (36a) and (36b). Crosses are approximate one material solution Eqs. (14) and (16).

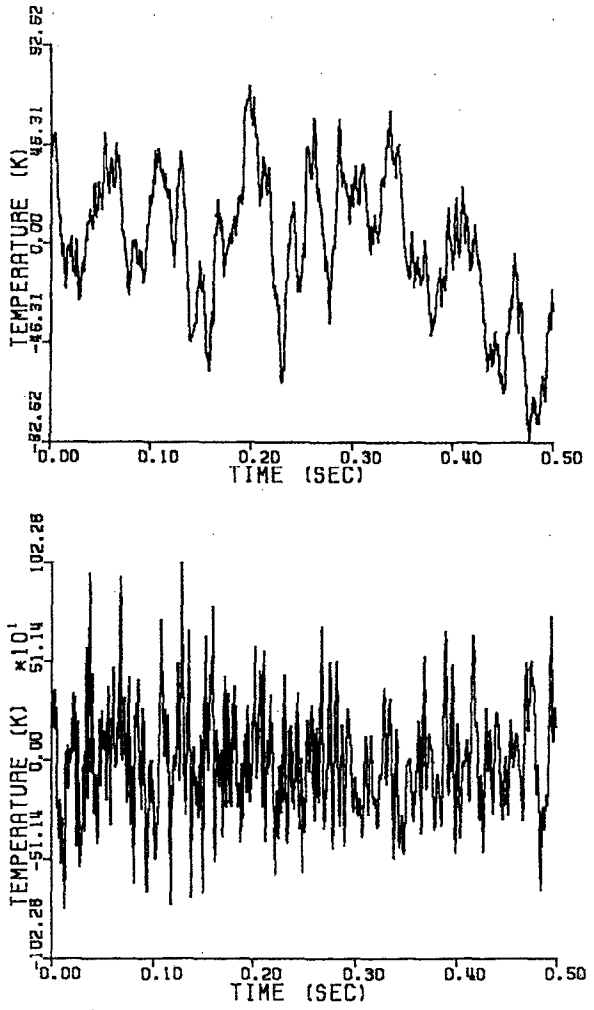

FIG. 10. Instantaneous temperature data taken with a Pt/6% Rh–Pt/30% Rh (type B) thermocouple. Dimensions: l=0.075 cm, L=0.15 cm, D_1=76 μm, and D_2=380 μm. The mean temperature of gas is 1452 K. Upper graph is uncompensated data with rms temperature of 33 K about mean. Lower graph is compensated data with rms temperature of 284 K.

D. Temperature compensation

Instantaneous temperature data were recorded in the high speed exhaust of a gas burner.[13] The uncompensated

data in the top graph of Fig. 10 represents one record taken with a type B thermocouple with the dimensions indicated in the caption. The fast Fourier transform was taken of the thermocouple signal (top of Fig. 10) and represented by $Y(\omega)$. The Fourier transform of the true gas temperature or $X(\omega)$ is given by

$$X(\omega)=\frac{Y(\omega)}{T(\omega)},$$

where $T(\omega)$ is Eq. (32). Thus, the true gas temperature (compensated data) is determined by taking the inverse transform of $X(\omega)$ or

$$T_g(t)=\mathrm{FFT}^{-1}[X(\omega)].$$

The compensated data or the estimate of the true gas temperature $T_g(t)$ is represented by the bottom graph of Fig. 10.

ACKNOWLEDGMENTS

The work reported herein was sponsored by the Air Force Systems Command (AFSC) under NASA cooperative agreement NCC 3-135 for the Arnold Engineering Development Center (AEDC), AFSC, Arnold Air Force Station, Tennessee. The contract officer is Ms. Marjorie Collier for the Directorate of Technology (DOT), AFSC. The authors also wish to acknowledge the support of Dr. W. D. Williams, head of the Research Sensor Technology Branch of NASA–Lewis and the helpful comments of Professor R. J. Moffat of Stanford University.

NOMENCLATURE

A = constant of integration
B = constant of integration
c = material specific heat ($\mathrm{J\,g^{-1}\,K^{-1}}$)
D = thermocouple wire diameter (cm)
G = $1+i(\omega/\omega_n)$
h = heat transfer coefficient ($\mathrm{J\,cm^{-2}\,s^{-1}\,K^{-1}}$)
i = unit imaginary number ($=\sqrt{-1}$)
k = material thermoconductivity ($\mathrm{J\,cm^{-1}\,s^{-1}\,K^{-1}}$)
k_f = gas thermoconductivity ($\mathrm{J\,cm^{-1}\,s^{-1}\,K^{-1}}$)
l = length of small thermocouple wire (cm)
L = length of large thermocouple wire (cm)
Nu = Nusselt number ($=hD/k_f$)
Pr = Prandl number ($=v_f/\alpha$)
Q = $D_1^2q_1/D_2^2q_2$
Q_t = k_1q_1/k_2q_2
Q_s = k_1q_3/k_2q_4
q = $(G/\gamma)^{0.5}$
Re = Reynolds number ($=vD/v_f$)
t = time (s)
T = steady-state frequency response
T_f = amplitude of periodic gas temperature (K)
T_g = gas temperature (K)
T_0 = mean gas temperature (K)
$\mathbf{T}_\omega$ = complex amplitude of periodic wire temperature (K)
T_w = local wire temperature (K)
v = gas velocity ($\mathrm{cm\,s^{-1}}$)
x = axial distance from center of wire (cm)

Greek symbols

α = thermal diffusivity ($\mathrm{cm^2\,s^{-1}}$)
γ = α/ω_n ($\mathrm{cm^2}$)
v_f = kinematic viscosity of gas ($\mathrm{cm^2\,s^{-1}}$)
ω = angular frequency ($\mathrm{s^{-1}}$)
ω_n = natural frequency of wire ($=4h/\rho cD$) ($\mathrm{s^{-1}}$)
Φ = phase angle
ρ = material density ($\mathrm{g\,cm^{-3}}$)
Δ_1 = dimensionless function
Δ_2 = dimensionless function

[1] R. R. Dils and P. S. Follansbee, *Wide Bandwidth Gas Temperature Measurements in Combustor and Combustor Exhaust Gases*, Instrumentation in the Aerospace Industry, Vol. 21, edited by B. Washburn, ISA ASI 76245 (1976).
[2] G. C. Fralick, Report No. NASA CP-2465, 1985, pp. 81–85.
[3] M. D. Scadron and I. Warshawsky, Report No. NACA TN-2599, 1952.
[4] D. L. Elmore, W. W. Robinson, and W. B. Watkins, Final Report No. NASA CR-168267, 1983.
[5] D. L. Elmore, W. W. Robinson, and W. B. Watkins Further, Report No. NASA CR-179513, 1986.
[6] L. J. Forney, E. Meeks, J. Ma, and G. C. Fralick, Final Report Georgia Tech E-19-666-4, NASA Cooperative Agreement No. NCC 3-135, October 1992.
[7] L. J. Forney, E. Meeks, J. Ma, and G. C. Fralick, Rev. Sci. Instrum. **64**, 1280 (1993).
[8] L. J. Forney and G. C. Fralick, Int. Comm. Heat Mass Transfer, **18**, 531 (1991).
[9] F. B. Hildebrand, *Advanced Calculus for Applications*, 2nd ed. (Prentice–Hall, Englewood Cliffs, NJ, 1976).
[10] *Thermal Physical Properties of Matter*, edited by Touloukian, Powell, Ho and Clemens, Purdue Research Foundation (Plenum, New York, (1970).
[11] J. Chomiak and B. Niedzialek, Int. J. Heat Mass Transfer **10**, 1571 (1967).
[12] D. R. Stocks, Report No. NASA CR-179604, 1986.
[13] G. C. Fralick, L. G. Oberle, and L. C. Greer, Report No. NASA TM-106119, 1993.